

Crack-resistance behavior as a consequence of self-similar fracture topologies

ALBERTO CARPINTERI and BERNARDINO CHIAIA

Dipartimento di Ingegneria Strutturale, Politecnico di Torino, Corso Duca degli Abruzzi 24, 10129 Torino, Italy

Received 20 April 1995; accepted in revised form 3 November 1995

Abstract. The effect of the invasive fractality of fracture surfaces on the toughness characteristics of heterogeneous materials is discussed. It is shown that the interplay of physics and geometry turns out to be the non-integer (fractal) physical dimensions of the mechanical quantities involved in the phenomenon of fracture. On the other hand, fracture surfaces experimentally show multifractal scaling, in the sense that the effect of fractality progressively vanishes as the scale of measurement increases. From the physical point of view, the progressive homogenization of the random field, as the scale of the phenomenon increases, is provided. The Griffith criterion for brittle fracture propagation is deduced in the presence of a fractal crack. It is shown that, whilst in the case of smooth cracks the dissipation rate is independent of the crack length a , in the presence of fractal cracks it increases with a , following a power law with fractional exponent depending on the fractal dimension of the fracture surface. The peculiar crack-resistance behavior of heterogeneous materials is therefore interpreted in terms of the self-similar topology of the fracture domains, thus explaining also the stable crack growth occurring in the initial stages of the fracture process. Finally, extrapolation to the macroscopic size-scale effect of the nominal fracture energy is deduced, and a Multifractal Scaling Law is proposed and successfully applied to relevant experimental data.

1. Introduction: fractality of the fracture surfaces

In the recent years, quantitative fractography has become an essential tool for the characterization of the breaking properties of disordered materials. The analysis of fracture surfaces often provides information about the micro- and meso-mechanical processes that cause the localization of strains and the final rupture in a material. An exhaustive treatise on the modern developments of fractography is provided in the paper by Coster and Chermant [1], where, for the first time, the possibility of applying Fractal Geometry to the quantitative characterization of fracture surfaces is addressed.

The first experimental attempt in this sense is that of Mandelbrot et al. [2], who determined the fractal dimension of steel fracture surfaces by means of the *slit island* method and subsequently related the computed values to the impact energy of the material. Other interesting references regarding fractality of metal fracture surfaces are [3-5]. In [6] fractality has been detected, up to the atomic scale (~ 40 nm), in the fracture surfaces of molybdenum. The interpretation of the stick-slip transition of natural faults and, in general, of the shear behavior of rock joints, calls for a synthetical modelization of the contact surfaces. Fractal Geometry has turned out to be a powerful tool for the description of rock discontinuities, as can be deduced from the literature [7, 8].

The application of the fractal concepts to cementitious materials is relatively recent with respect to the case of rocks and metals, but has immediately proved to be a very appropriate approach, due to the *multi-scale heterogeneity* of these materials. The hierarchical microstructure of concrete, in fact, ranges from the microscopic level of the cement clinker (siliceous phases embedded in the aluminium-ferritic matrix) to the mesoscopic level of the mixture

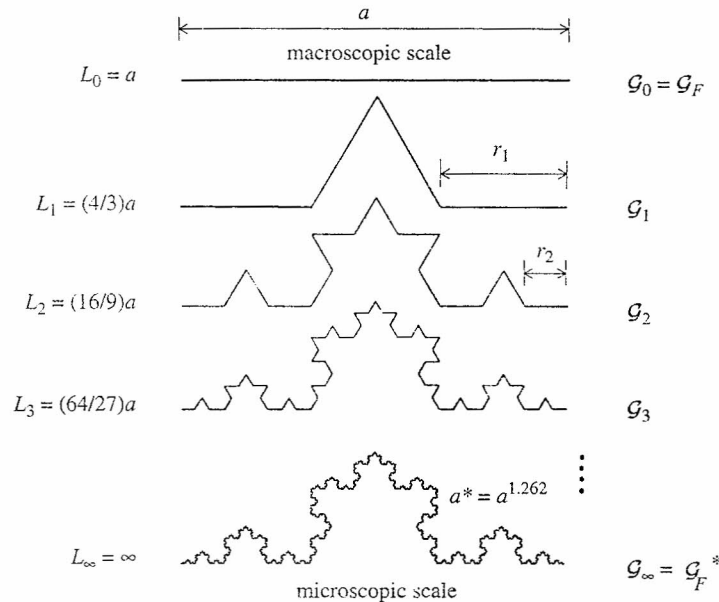


Figure 1. Invasive self-similarity: the von Koch curve ($\Delta = 1.262$).

(distribution of pores in the mortar), up to the macroscopic level (coarse aggregates embedded in the paste). The first experimental attempt to determine the fractal characteristics of concrete fracture surfaces is that of Saouma et al. [9], who detected anomalously low values of the fractal dimension Δ due to the self-affine character of the considered domains. Lange [10], Issa and Hammad [11], and Carpinteri and Chiaia [12] also investigated concrete fracture surfaces by means of different experimental techniques, always proving the fractality (that is, topological self-similarity) of the fracture domains.

The fundamental aspect to be pointed out regards the physical significance of fractality. The deep connection between physics and topology is nowadays well known in the framework of critical phenomena. Physical systems undergoing catastrophic transformations, like phase transitions, earthquakes and brittle fracture, show at the critical point fluctuations that are *self-similar* at all length scales, thus resulting in the (theoretical) absence of any internal characteristic length (or, which is the same, in the infinite correlation length of the phenomenon). In the case of fracture surfaces, invasive fractals (i.e. fractal domains with topological dimension Δ strictly larger than their Euclidean projection) are supposed to be adequate models for their topology. The von Koch curve (Figure 1), for example, can be considered the archetype of fracture trajectories, that is, of fracture profiles obtained as intersections of the fracture surface with orthogonal planes.

On the other hand, some conceptual mistakes can be evidenced in the literature. First of all, fractality has often been misinterpreted as a merely morphological occurrence [9], in the sense that the fractal dimension Δ has been used for quantifying surface roughness just like other typical roughness parameters (*Joint Roughness Coefficient*). Another misunderstanding [7] is that of considering a nominal area (physical dimension = $[L]^2$) of the fracture surface, increased with respect to the area of its projection, instead of considering the proper measure of the fractal set, which is a *non-integer measure* (physical dimension = $[L]^\Delta$, $\Delta > 2$) [12]. Note that this corresponds to modeling the fracture domain as a simple stage in the iterative

definition of a fractal set (Figure 1), instead of properly modeling it as the fractal set itself, which is a limit concept. Such confusion turns out to be the definition of mechanical properties (fracture energy \mathcal{G}_F , shear strength τ_u) that are quantitatively modified due to the increased area, but are still erroneously defined on Euclidean sets.

Therefore, positive correlation between values of toughness and fractal dimension has been hypothesized by many authors [4]. On the other hand, after an extensive statistical investigation on various experimental data, Davidson [13] showed that no correlation can be consistently stated in this way, and that the influence of the fractality of the fracture surfaces on the mechanical properties of the material has to be caught in a dramatically different sense. It can be affirmed that, due to the fractional measurability of fractal sets, all the mechanical quantities that are defined over these domains have to take anomalous (non integer) physical dimensions [14]. Only in this way is it possible to obtain physical quantities that are *universal*, that is, scale-independent, and to explain some peculiar aspects in the breaking behavior of disordered materials, like the size-effect on the nominal fracture energy and the nonlinear crack-resistance behavior.

2. Geometrical multifractality: transition from Brownian disorder to Euclidean order

The experimental investigations on the concrete fracture surfaces have often provided anomalously low values [5, 9]. It can be argued that this is due to the essential difference between mathematical and natural fractal sets. All the fractal sets in nature show *random* self-similar morphologies in the sense that their aspects look *statistically* (and not exactly, as in the case of mathematical fractals) the same by changing the scale of observation.

Besides randomness, two more aspects have to be explained that are peculiar for all the natural fractal structures: first of all, the presence of an upper and a lower bound in the scaling range and, consequently, *the inevitable transition from the fractal (disordered) regime at the microscopic scales towards an Euclidean (homogeneous) regime at the largest scales*. The upper bound is represented by the macroscopic size b of the domain, whilst the lower one is related to the size of the smallest measurable particles, these being the grains, in the case of metals, the crystals, in the case of rocks, and the aggregates in the case of concrete. It can be argued that the presence of an *internal characteristic length* l_{ch} , typical of each microstructure, inhibits the development of a perfect self-similar scaling through the whole scale range, whereas mathematical fractals like the von Koch curve in Figure 1, lacking absolutely any characteristic length, exhibit uniform (monofractal) scaling without any bound. Therefore, all the numerical tools for the determination of the fractal dimension have to be properly modified in order to take into account this peculiar character of the fracture surfaces, otherwise only the Euclidean regime will be detected [15].

Mandelbrot first [16] pointed out the transition from a fractal regime, characterized by non-integer dimensions, to the homogeneous one, characterized by the classical Euclidean dimensions, defining '*self-affinity*' as non-uniform scaling of natural fractals. Experimental investigations carried out by the authors [12] on laser-digitized concrete fracture profiles showed that the two regimes are only the asymptotics of a continuous topological transition. Measurements of fractal dimension have been carried out by means of the Box-Counting Method (Figure 2) and of the Spectral Method. In the first case, by considering the logarithmic density of the Euclidean coverings as the measurement scale tends to zero, the fractal dimension Δ_{Box} of the profile (which can be considered equal to the fractal dimension Δ of the surface minus one) is obtained as

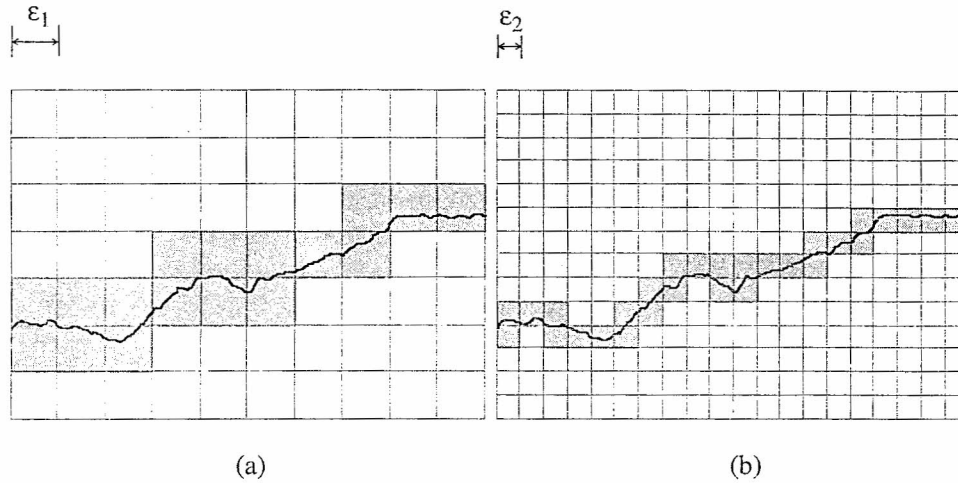


Figure 2. Box-Counting Method: coverings of a fractal profile.

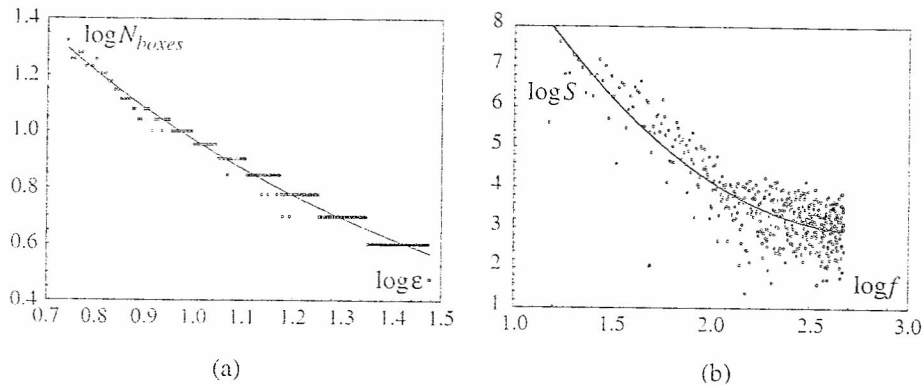


Figure 3. Fractal analysis of a fracture trajectory by the Box-Counting Method (a) and by the Spectral Method (b).

$$\Delta_{\text{Box}} = 2 - \lim_{\varepsilon_i \rightarrow 0} \frac{\log(E_i)}{\log \varepsilon_i} = \lim_{\varepsilon_i \rightarrow 0} \frac{\log(N_i)}{\log(1/\varepsilon_i)}, \quad (1)$$

where E_i is the area of the shaded cover, built by means of N_i boxes with linear size ε_i in order to entirely cover the fracture profile. In Figure 3(a) the application to a fracture profile is shown: note the upward concavity of the best-fitting curve, which does not allow for determining a unique slope, that is, a unique fractal dimension (a monofractal set would have yielded a straight line in the bilogarithmic diagram, and (1) would have been applied).

Results by the Spectral Method are shown in Figure 3(b): in this case the power spectral density obtained by Fourier transform of the profile is plotted versus the spatial frequency, thus extracting the degree of spatial correlation in the fracture domain. The fractal dimension Δ_S , in the monofractal hypothesis, would be given by

$$\Delta_S = \frac{5 - \beta}{2}, \quad (2)$$

where β is the slope of the best-fitting line in the bilogarithmic diagram. Note, also in this case, the upward concavity in the plot, which implies the progressive vanishing of fractality as the spatial frequency decreases, that is, as the scale of observation increases.

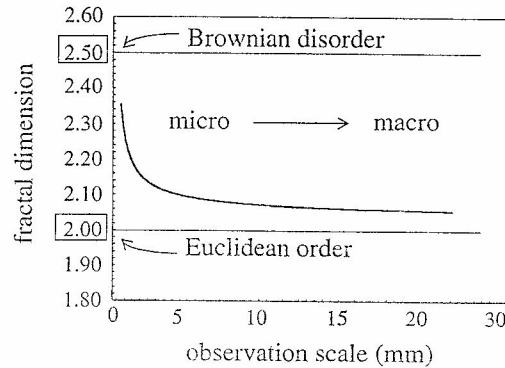


Figure 4. Geometrical multifractality of the fracture surfaces.

Therefore, it has been proposed by the authors [12] to define this kind of scaling as *geometrical multifractality*, since an infinity of exponents is necessary in order to describe the entire range of the scaling (Figure 4). As will be demonstrated in the following, from the physical point of view, this anomalous scaling essentially provides the *progressive vanishing of the effect of microstructural disorder on the mechanical properties of the material as the scale of the phenomenon increases* [17].

Moreover, the aforementioned investigations showed that the highest possible disorder in the fracture surfaces is represented by a *Brownian disorder*, in the sense that a fractal dimension equal to 2.5 seems to be the highest in the limit of microscopic scales of observation. Such a thermodynamic assumption (Brownian motion is the archetype of dissipative phenomena) is confirmed by the multitude of fractal dimension measurements in different materials that have been reported in the literature, and by the suggestive hypothesis that Brownian surfaces would globally minimize the energy dissipation [18]. On the other hand, as will be shown in the last section, an indirect validation of this assumption comes from the experimental determination of the scaling exponents for the nominal fracture energy size-dependence, that have never been measured larger than $+\frac{1}{2}$.

3. The Griffith fractal crack

The well-known Griffith criterion for brittle fracture propagation [19] can be extended to the case of fractal fractures. Instead of the classical smooth Griffith crack (with length $2a$ and Euclidean dimension equal to 1 in the bidimensional plane, (Figure 5(a)), let us consider a fractal crack with projection $2a$ and fractional dimension $\Delta_G > 1$, embedded in an infinite plate subjected to uniform traction (Figure 5(b)). For the sake of simplicity, let us initially assume a monofractal deterministic domain: note that these hypotheses do not make the treatise lose generality, since extension to random fractals is trivial and multifractality will be considered next.

Taking, due to the symmetry, only one-half of the plate (Figure 6), and recalling the basic relations from fractal geometry, if we consider the crack as a fractal set a^* , with projected length a and fractal dimension $\Delta_G = 1 + d_G$, the following fundamental relation holds

$$N_n r_n^{\Delta_G} = a^{\Delta_G}, \quad (3)$$

where $n = 1, 2, \dots, \infty$ is the iteration scale (Figure 1), a is the projected length, also called *initiator*, r_n is the scaling factor of lengths at scale n and N_n represents the number of

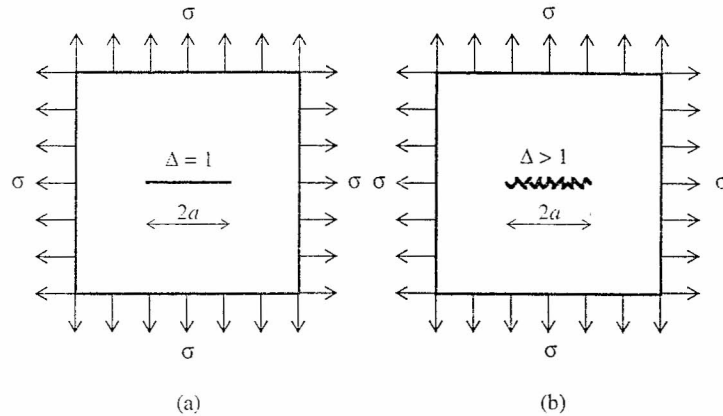


Figure 5. Infinite sheet subjected to uniform tractions and containing a smooth (a) and a fractal (b) crack.

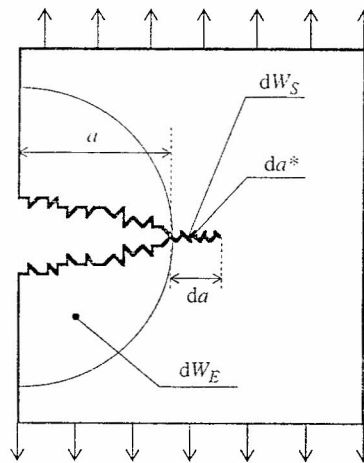


Figure 6. Griffith instability in the presence of a fractal crack.

segments at scale n . Equation (3) states the self-similarity of the fracture domain through the whole range of measurement scales. The nominal length L_n of the fractal profile, measured at scale n , that is, computed by means of a yardstick length r_n walked along the profile, is equal to $N_n r_n$ and from (3) to

$$L_n = a^{(1+d_G)} r_n^{(-d_G)}. \quad (4)$$

One can easily verify that in the limit of $r_n \rightarrow 0$, that is, in the limit of the smallest scales of observation, this fictitious length tends to infinity. The above circumstance is a fundamental feature of fractal geometry: all the attempts made in order to define any physical quantity over a finite length value of a fractal set must be considered as conceptual mistakes. More and more irregularities are computed as the measurement scale decreases, and no geometric tangent can be unequivocally associated with any point of the profile: this expresses the well-known characteristic of fractal sets to be *non-differentiable* (in a classical sense) mathematical objects.

The fundamental Griffith relation of energy balance, at the critical point of unstable crack propagation, states

$$\frac{dW_E}{da} = \frac{dW_S}{da}, \quad (5)$$

where the first term represents the elastic energy release rate due to the propagation (equal to $2da$ in the horizontal projection) of the pre-existing fractal crack, and dW_S is the total energy dissipated on the developing fractal crack, due to the breaking of the material bonds and the coalescence of microcracks. The elastic energy release is a macroscopic and global parameter, being defined in the bulk, which means that it is independent of the observation scale: it is therefore not sensitive to disorder, so that fractality does not come into play in its definition. On the contrary, dW_S represents the energy directly dissipated in the fractal domain, and thus the *nature* of this dissipation is intimately controlled by the disordered microstructure. On the other hand, due to the requested dimensional homogeneity in (5), the global quantity dW_S holds the usual physical dimensions of an energy ($[F][L]$). In the case of a smooth crack the following relations hold [19]

$$\frac{dW_E}{da} = \frac{d}{da} \left(\frac{\sigma^2 \pi a^2}{E} \right) = \frac{2\pi \sigma^2 a}{E}, \quad (6a)$$

$$\frac{dW_S}{da} = 4\gamma = 2\mathcal{G}_F, \quad (6b)$$

where $\gamma([F][L]^{-1})$ represents the surface energy dissipated on each face of the opening crack. By substituting (6a) and (6b) in the balance relation (5), and defining the ‘fracture energy’ \mathcal{G}_F of the material as $\mathcal{G}_F = 2\gamma$, the well-known Griffith criterion for brittle fracture is obtained:

$$\sigma \sqrt{\pi a} \leq \sqrt{\mathcal{G}_F E}, \quad (7)$$

which can be expressed, following Irwin’s demonstration [20], in terms of the stress-intensity factor, as $K_I \leq K_{IC}$, where K_{IC} is the *critical stress-intensity factor* or the *fracture toughness* of the material.

In the case of a fractal crack, we assume that at each scale of observation n , a nominal *microscopic* fracture energy \mathcal{G}_n is dissipated along a nominal length L_n : the rate of energy dissipated *at this scale* as each crack tip moves the infinitesimal projected quantity da (Figure 6), is therefore given by

$$\left[\frac{dW_S}{da} \right]_n = 2 \frac{d(\mathcal{G}_n L_n)}{da}. \quad (8)$$

In order to obtain a scale-independent value, since the fractal set is by definition a limit concept, (i.e. the set of points corresponding to the scale of observation tending to zero), and recalling (4), we can write

$$\frac{dW_S}{da} = 2 \times \lim_{n \rightarrow \infty} \left(\frac{d(\mathcal{G}_n L_n)}{da} \right) = 2(1 + d\mathcal{G}) a^{d\mathcal{G}} \left[\lim_{n \rightarrow \infty} \left(\mathcal{G}_n r_n^{(-d\mathcal{G})} \right) \right]. \quad (9)$$

Note that the expression inside the square brackets is indeterminate since it results in a form $0 \times \infty$. The key of the above procedure is to solve the limit in (9) by invoking the

Renormalization Group Theory [21], which allows one to define finite *renormalized* physical quantities as the fixed points of the scaling transformations, at the cost of abandoning canonical dimensions

$$\lim_{n \rightarrow \infty} \left(\mathcal{G}_n r_n^{(-d_{\mathcal{G}})} \right) = \mathcal{G}_F^*. \quad (10)$$

From the above relation the non-integer physical dimensions ($[F][L]^{-(1+d_{\mathcal{G}})}$) of the *renormalized fracture energy* are provided, depending on that of the dissipation fractal space. Inserting (10) into (9), the following fundamental expression is obtained

$$\frac{dW_S}{da} = 2(1 + d_{\mathcal{G}}) \mathcal{G}_F^* a^{d_{\mathcal{G}}}. \quad (11)$$

The procedure exposed from (8) to (11) represents a physically-justified methodology in order to by-pass the formal non-differentiability of fractal sets. The rate of change of a physical quantity defined on a fractal space is provided by an ordinary analytical derivative taken in correspondence to the generic observation scale, which then turns into a scale-independent value by means of the Renormalization Group. Similar results have been obtained by Mosolov [22], without realizing, indeed, the mechanical consequences of the fractional dimensionality.

It is interesting to note that (11) can be deduced by directly considering the *renormalized (fractal) fracture energy* \mathcal{G}_F^* , and taking the simple derivative of a^* with respect to a , where $a^* = a^{(1+d_{\mathcal{G}})}$ is the ‘measure’ (in the Hausdorff sense) of the fractal set. This means that the *mass* (in a topological sense) of the fractal domain can be unequivocally (that is, scale-independently) obtained only by measuring it by means of length raised to $(1 + d_{\mathcal{G}})$. In this context one can simply write:

$$\frac{dW_S}{da} = 2 \mathcal{G}_F^* \frac{d(a^*)}{da} = 2(1 + d_{\mathcal{G}}) \mathcal{G}_F^* a^{d_{\mathcal{G}}}, \quad (12)$$

which exactly corresponds to (11). This procedure could be called ‘*projective derivative*’, and arises from the relation between fractal and classical coordinates. Classical coordinates come into play when the fractal space is smoothed by means of balls of radii greater than some critical value, that is, looking at the fractal ‘from outside’. As can be easily seen in (12), the intersection of a regular fractal a^* of dimension $\Delta_{\mathcal{G}} = 1 + d_{\mathcal{G}}$ with a D -manifold ($D = 1$ in our case) is another fractal, the *projective derivative* of a^* , with dimension $\Delta_{\mathcal{G}} - 1$.

Based on (11) or (12), the energy balance relation (5), in the case of fractal cracks, yields

$$\sigma^2 \pi a^{(1-d_{\mathcal{G}})} = (1 + d_{\mathcal{G}}) \mathcal{G}_F^* E, \quad (13)$$

which can be expressed, as in the smooth case, in terms of the stress-intensity factor as $(K_I^*)^2 = (K_{IC}^*)^2$, where the *fractal stress intensity factor* presents the following anomalous physical dimensions

$$[K_I^*] = [F][L]^{-((3+d_{\mathcal{G}})/2)}. \quad (14)$$

Generalizing Irwin’s solution, the near-tip elastic stress field can be written as

$$\sigma_{ij} = K_I^* r^{-((1-d_{\mathcal{G}})/2)} f_{ij}(\theta), \quad (15)$$

where the power of the singularity strictly depends on d_G . The invasive dimensionality of the crack provides an attenuation of the fracture localization, involving also an attenuation of the stress singularity and, macroscopically, a more ductile behaviour of disordered materials. When $d_G = 0$, we find again the classical relations of Griffith and Irwin. When $d_G = 1$, as a limit case, we find that the stress singularity at the crack tip vanishes and K_I^* assumes the physical dimensions of stress. Therefore no localization occurs, as if the energy were dissipated in the bulk ($\Delta_G = 3$).

4. *R*-curve behavior of heterogeneous materials

A connection between structural response and crack-growth resistance curve has been established by one of the authors [23] by relating the relevant parameters of a scale-invariant *J*-resistance curve to the energy brittleness number. By means of dimensional analysis arguments, the size-scale transition from ductile to brittle fracture has been captured according to the *J*-resistance approach. From a physical point of view, abandoning the *complete* similarity of the Euclidean topologies permits moving to the *incomplete* similarity of the fractal domains [17]. A fundamental consequence of the fractality of the fracture surfaces, physically related to the smoothing of the stress-singularity, comes from the comparison between (6b) and (11): while in the case of smooth cracks the energy dissipation is independent of a , being constant during crack propagation, in the presence of fractal cracks it increases with a , following a power-law with fractional exponent equal to d_G . If the nominal fracture energy is related to the renormalized one, it is easy to obtain

$$\mathcal{G}_F \approx \mathcal{G}_F^* a^{d_G}, \quad (16)$$

which clearly indicates that the presence of disorder introduces nonlinearity in the fracture behaviour of a linear elastic material. What is usually considered as a material constant during crack propagation, turns out to be an increasing function of the crack length (Figure 7(a)), thus implying that the *crack resistance grows during the propagation of the fractal crack* (*R*-curve behavior).

Gong and Lai [24], based on early suggestions by Williford [25], have given analogous interpretation of the experimentally determined *J*-*R* resistance curves of Ti-6Al-4V alloys. Assuming that the *J*-integral crack-growth criterion were satisfied, and that the fracture paths were fractal, they derived the following relation between the specific work *J* required for the crack propagation and the crack advancement Δa

$$J = C(\Delta a)^{\Delta_G - 2}, \quad (17)$$

where the constant *C* is related to γ (surface energy dissipated per unit area of crack growth) and to s , which is an arbitrary small scale of length. Although this empirical approach fits the problem well, it should be pointed out that the physical essence of fractality is disregarded, since the deep significance of the fractional dimensionality is not taken into account.

On the other hand, one can easily notice that (16) and (17) would yield infinite toughness as the crack extends, which is obviously far from the experimental reality. This is owing to the modelization of the Griffith crack by means of a mathematical fractal, that is, a monofractal. Recalling the experimental evidence of the multifractality of the fracture surfaces (Figure 4), it can be argued that the relevance of fractality decreases as the crack propagates (that is, as the crack extension a becomes larger and larger with respect to some microstructural characteristic

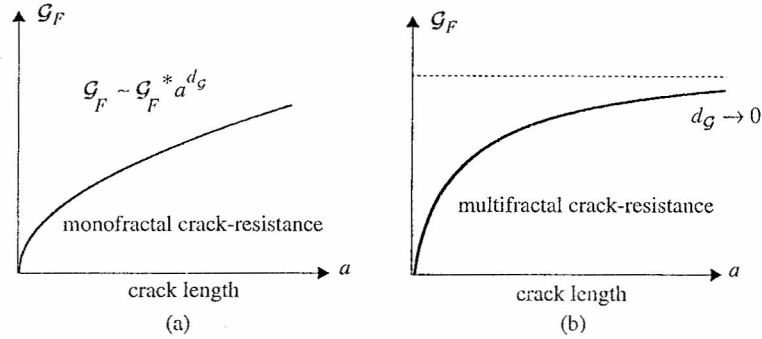


Figure 7. Crack-resistance behavior in the monofractal (a) and multifractal (b) hypotheses.

length l_{ch}). Therefore, it can be stated that d_G progressively tends to zero as the crack extends, thus implying, in (16), an horizontal asymptote for the fracture toughness (Figure 7(b)), in perfect agreement with the experimental observations, where a *plateau* in the crack-resistance behavior is always detected. From the theory of the fractal Griffith crack, this means that the power α of the stress singularity at the tip of the moving crack increases during propagation, yielding the LEFM behavior ($\alpha \rightarrow \frac{1}{2}$) only after a certain extension.

The fractal crack-resistance behavior matches satisfactorily the experimental data obtained by means of several fracture tests on concrete specimens, and permits explaining the initial *stable crack growth* that is usually encountered when analyzing the fracture properties of heterogeneous materials. Note that, according to the *R-curve* theory usually applied to metals, the nonlinear crack-resistance behavior is provided by the constitutive laws of the material, whereas, according to the fractal approach, it is derived from the topological *space-filling* ability of the fracture domains, which in turn is due to the microstructural disorder.

The fractal interpretation of the *R-curve* behavior agrees with the classical approach of Wittmann et al. [26], who state that responsibility for the crack resistance increase during propagation is the progressive dilatation of the fracture process zone (FPZ) width a_p , which causes the increase of the critical crack opening displacement $w_2 = w_c$ in a bilinear cohesive law (Figure 8). Since the energy dissipation takes place in the fracture process zone, if its width expands during crack propagation up to a limit value $(w_2)_{lim}$ (*fully-developed process zone*), it is reasonable to suppose that once the FPZ attains its highest width and remains constant, the highest value of w_c is reached, yielding the highest *local* fracture energy as an asymptotic. The authors define a *local fracture energy* $g_F(x)$, proportional to the FPZ width, whose integration along the fracture path provides a size-dependent fracture energy, thus explaining in this way also the size-scale effect on the nominal fracture energy \mathcal{G}_F , which is addressed in the next section.

5. Size-scale effect on nominal fracture energy

As often occurs in natural phenomena, the physical laws controlling the phenomenon at the micro- or meso-level determine an analogous behavior at the macroscopic scale. One could easily recognize in (11), the 'shell' of the monofractal size-scale effect on the nominal fracture energy as has been interpreted by Carpinteri [14]. Extrapolating, in fact, the scaling behavior of \mathcal{G}_F from the meso-level up to the structural macro-level, if b is a reference dimension of

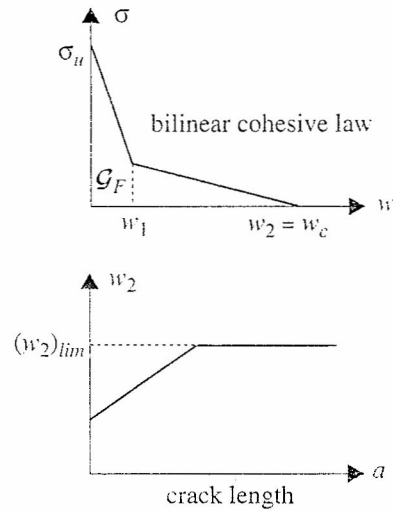


Figure 8. Bilinear cohesive law (a) and evolution of the FPZ according to [26].

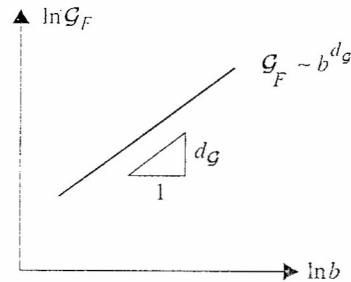


Figure 9. Size effect on the nominal fracture energy (monofractal hypothesis).

the structure, the nominal fracture energy increases with size yielding a slope equal to d_G in the bilogarithmic diagram $\log \mathcal{G}_F$ vs. $\log b$ (Figure 9).

As in the case of the crack-resistance, an infinite value of fracture energy would be provided for the larger sizes, which is evidently not corresponding to reality. Therefore, taking into account the multifractality of the fracture domains, a Multifractal Scaling Law (MFSL) for the nominal fracture energy \mathcal{G}_F has been proposed by the authors [15]. The analytical expression for the Multifractal Scaling Law, represented in Figure 10, is the following

$$\mathcal{G}_F(b) = \mathcal{G}_F^\infty \left[1 + \frac{l_{ch}}{b} \right]^{-1/2}, \quad (18)$$

where \mathcal{G}_F^∞ is the nominal asymptotic fracture energy, valid in the limit of infinite structural size ($b \rightarrow \infty$), and l_{ch} is the value of a characteristic internal length, which controls the transition from the fractal regime to the Euclidean one. The non-dimensional term into square brackets represents the decrease, due to the disorder, of the nominal fracture energy with respect to the constant asymptotic value. Note that the hypothesis of Brownian motion as an upper limit for the microscopic disorder is satisfied by the former expression: if one takes the derivative of (18), and considers its limit for $b \rightarrow 0^+$, the maximum slope of the size effect law, equal to $+\frac{1}{2}$, is obtained. On the basis of the MFSL, the RILEM fracture energy [27],

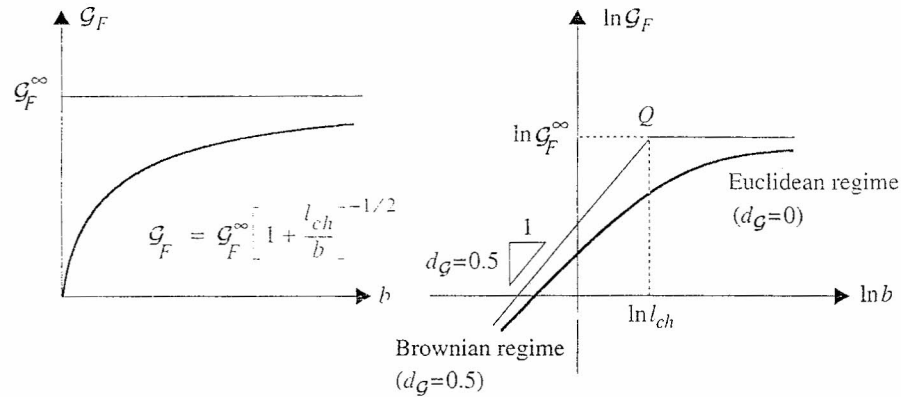


Figure 10. Multifractal Scaling Law for the nominal fracture energy.

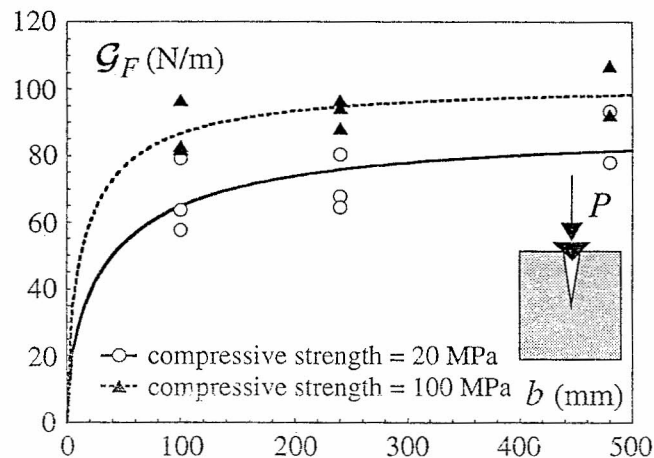


Figure 11. Application of the MFSL to the data by Kim et al. [28].

defined as a mean-field quantity, appears to be a physically meaningful parameter only in the homogeneous regime, whereas linear elastic fracture mechanics, characterized by a local approach (K_I), governs the collapse of unnotched structures only when the characteristic size a of microstructural defects becomes comparable with the macroscopic size b of the specimen or, as is the same, when the influence of disorder becomes essential (sufficiently small specimens). Note that this implies a dimensional transition of toughness, which can be reconducted to the non-integer dimensions of the renormalized fracture energy \mathcal{G}_F^* [14].

The Multifractal Scaling Law can be applied in order to interpret the results of experimental tests on different concrete geometries. From an engineering point of view, the method allows for the extrapolation, from laboratory-sized specimens, to a reliable value of the fracture energy valid for real-sized concrete structures.

Kim et al. [28] performed wedge-splitting tests on concrete with different compressive strengths and maximum aggregate size equal to 7 mm, detecting a strong dependence of the nominal fracture energy on the specimen size (size range = 1 : 5). The nominal fracture energy is obtained as the total work of fracture (computed from the load-displacement diagram) divided by the initial ligament. In Figure 11 the application of the MFSL to the experimental data is shown: in the case of the 20 MPa concrete, nonlinear fitting yields the asymptotic

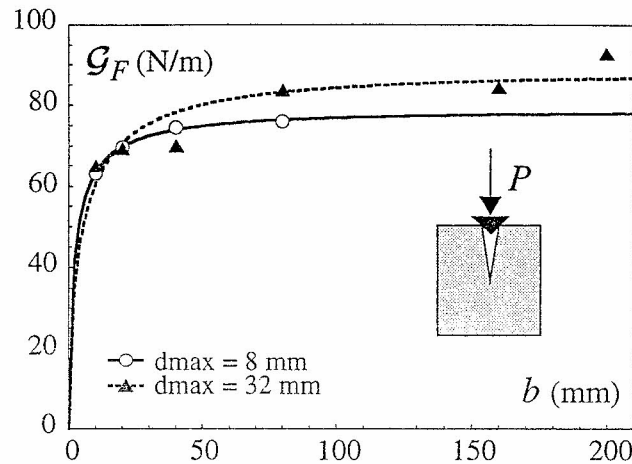


Figure 12. Application of the MFSL to the data by Zhong [29].

fracture energy $\mathcal{G}_F^\infty = 88.3 \text{ N/m}$, and the characteristic internal length $l_{ch} = 86.1 \text{ mm}$, whereas, in the case of the 100 MPa concrete, the following parameters are determined: $\mathcal{G}_F^\infty = 102.1 \text{ N/m}$ and $l_{ch} = 38.9 \text{ mm}$. Note that, even if the asymptotic fracture energy, in the case of the stronger mixture, is larger than in the case of the 20 MPa concrete, the internal length is smaller, thus indicating the more rapid homogenization (vanishing of fractality) occurring in the scaling behavior of the stronger concrete.

Zhong [29] performed wedge-splitting tests on two series of concrete with different maximum grain size, 8 mm and 32 mm, respectively. The examined size range is (1:8) in the case of the finer mixture and (1:20) in the case of the coarse one. In Figure 12 the application of the MFSL to the experimental data is shown: in the case of the finer grained concrete, nonlinear fitting yields the asymptotic fracture energy $\mathcal{G}_F^\infty = 78.9 \text{ N/m}$, and the characteristic internal length $l_{ch} = 5.6 \text{ mm}$, whereas, in the case of the coarse grained concrete, the following parameters are determined: $\mathcal{G}_F^\infty = 89.1 \text{ N/m}$ and $l_{ch} = 11.8 \text{ mm}$. As expected, concrete with a larger maximum aggregate size has a higher asymptotic fracture energy. Moreover, it is interesting to point out that the coarse mixture yields a larger internal length, according to the MFSL, and therefore the transition to the homogeneous behavior occurs later than in the case of the 8 mm mixture. It is therefore confirmed that the value of l_{ch} is intimately related to the maximum aggregate size, as has been previously supposed by the authors: $l_{ch} = \alpha d_{\max}$, where α is a dimensionless constant of proportionality [15].

Acknowledgements

The present research was carried out with the financial support of the Ministry of University and Scientific Research (MURST) and the National Research Council (CNR).

References

1. M. Coster and J.L. Chermant, *International Metals Review* 28 (1983) 228–250.
2. B.B. Mandelbrot, D.E. Passoja and A.J. Paullay, *Nature* 308 (1984) 721–722.
3. C.S. Pande, L.R. Richards and S. Smith, *Journal of Material Science Letters* 6 (1987) 295–297.
4. E.E. Underwood and K. Banerji, *Materials Science and Engineering* 80 (1986) 1–14.
5. C.W. Lung and S.Z. Zhang, *Physica D* 38 (1989) 242–245.
6. H. Sumiyoshi, S. Matsuoka, K. Ishikawa and M. Nihei, *JSME International Journal* 35 (1992) 449–455.

7. H. Xie, in *International Symposium on Application of Computer Methods in Rock Mechanics and Engineering*, A.A. Balkema Publishers, Amsterdam (1993).
8. S.R. Brown and C.H. Scholz, *Journal of Geophysical Research* 90 (1985) 12575–12582.
9. V.E. Saouma, C.C. Barton and N.A. Gamaleldin, *Engineering Fracture Mechanics* 35 (1990) 47–53.
10. D.A. Lange, H.M. Jennings and S.P. Shah, *Journal of American Ceramic Society* 76 (1993) 589–597.
11. M.A. Issa and A.M. Hammad, *Cement and Concrete Research* 24 (1994) 325–334.
12. A. Carpinteri and B. Chiaia, *Materials and Structures* 28 (1995) 435–443.
13. D.L. Davidson, *Journal of Materials Science* 24 (1989) 681–687.
14. A. Carpinteri, *Mechanics of Materials* 18 (1994) 89–101.
15. A. Carpinteri and B. Chiaia, *Materials and Structures* (1996), to be published.
16. B.B. Mandelbrot, *Physica Scripta* 32 (1985) 257–260.
17. A. Carpinteri, *International Journal of Solids and Structures* 31 (1994) 291–302.
18. A. Chudnowski and B. Kunin, *Journal of Applied Physics* 62 (1987) 4124–4133.
19. A.A. Griffith, *Philosophical Transaction of the Royal Society* (London), A221 (1921) 163–198.
20. G.R. Irwin, *Journal of Applied Mechanics* 24 (1957) 361–364.
21. K.G. Wilson, *Physical Review B* 4 (1971) 3174–3205.
22. A.B. Mosolov, *Europhysics Letters* 24 (1993) 673–678.
23. A. Carpinteri, *International Journal of Fracture* 51 (1991) 175–186.
24. B. Gong and Z.H. Lai, *Engineering Fracture Mechanics* 44 (1993) 991–995.
25. R.E. Williford, *Scripta Metallurgica et Materialia* 24 (1990) 455–460.
26. F.H. Wittmann, H. Mihashi and N. Nomura, *Engineering Fracture Mechanics* 35 (1990) 107–115.
27. RILEM Technical Committee 50, *Materials and Structures* 18 (1985) 287–290.
28. J.K. Kim, H. Mihashi, K. Kirikoshi and T. Narita, in *Proceedings of the First International Conference on Fracture Mechanics of Concrete Structures*, FRAMCOS1, Breckenridge (1992) 561–566.
29. H. Zhong, Internal Report, Institute for Building Materials, Swiss Federal Institute of Technology, Zürich, (1991).